Theoretical study of space focusing in linear time-of-flight mass spectrometers

D. P. Seccombe[a] and T. J. Reddish[b]
Physics Department, Newcastle University, Newcastle-upon-Tyne, NE1 7RU, United Kingdom

(Received 15 August 2000; accepted for publication 2 November 2000)

In response to continued improvements in the production of ''cold'' atoms, molecular beams, and in electronic timing resolution, the issue of space focusing in linear time-of-flight (TOF) mass spectrometers is reevaluated. Starting with the Wiley–McLaren [W. C. Wiley and I. H. McLaren, Rev. Sci. Instrum. **26**, 1150 (1955)] condition for first-order space focusing in the conventional two-field system, we extend the approach to higher orders in more complicated situations. A general, solvable, set of equations for satisfying *n*-order space focusing in an *m*-field regime is derived. We demonstrate quantitatively that if higher orders of space focus are employed, then provided the initial velocity distribution of the ions is sufficiently narrow, a significant improvement in the mass resolution can be achieved. The conclusions drawn have important implications for the design of the next generation of TOF instruments. © *2001 American Institute of Physics.*
[DOI: 10.1063/1.1336824]

I. INTRODUCTION

Time-of-flight (TOF) mass spectrometry is a well-established and widely used technique for determining the identities, relative concentrations, and energies of ions. The simplest system consists of an acceleration region followed by a field-free ''drift'' region, which together disperses the ions' ''time-of-flight'' according to their mass and charge. Over the years there have been significant improvements in the basic design, some of which invoke substantial changes in geometry to optimize the mass resolution. A variety of approaches have been used, including sector analyzers,[1–3] the ''reflectron'' design,[4,5] quadratic extraction fields,[6,7] time-dependent extraction fields—so-called ''impulse-field focusing,''[8,9] and the employment of additional parabolic reflectors to improve detection efficiency.[10] A review of TOF methods has been undertaken by Price and Milnes.[11] The widespread use of this technique has led to exotic applications such as analyzing the dust in the tail of Halley's comet,[12] imaging Bose–Einstein condensation,[13] and identifying biological materials with high mass numbers ($\sim 10^{12}$).[14]

The traditional limitations to the mass resolution have been due to the velocity and spatial distributions of the source. The simplest gas sources, provided by effusive beams, suffer from a broad, Maxwell–Boltzmann velocity spread that can dominate over the effects of the ion source's spatial extent. Wiley and McLaren[15] introduced ''space focusing,'' which endeavors to ensure that the ion time of flight is independent of small changes in initial position. As we have already alluded, this insensitivity is very important because in any practical situation the interaction region will have a finite size and so limit the mass resolution. First-order space focusing is often sufficient to accommodate the velocity spread associated with thermal ions. However, there has been considerable experimental effort over the years to reduce the velocity distribution of the ions. The use of supersonic beams in ionization experiments is one method that results in a much smaller transverse velocity spread. Another example is the use of laser cooling techniques leading to very ''cold'' trapped atoms with temperatures down to ~ 1 μK—or colder in the case of Bose–Einstein condensation.

With these reductions in the velocity spread, it is timely to reexamine the simple linear TOF design and to optimize its space-focusing characteristics. Its relatively simple yet highly efficient design can detect particles over 4π sr. It can also be used easily in conjunction with other types of particle analyzers, enabling coincidence experiments. Consequently, the linear TOF geometry is still widely employed and continues to be developed. For example, the cold-target recoil-ion mass spectrometry technique has been developed by Schmidt–Böcking and his co-workers over the last ten years.[16] This ''momentum imaging'' method, used in both photoionization and collision-induced ionization processes, detects an emitted electron and employs a precooled localized supersonic beam to optimize the momentum resolution of the detected recoil ion. This elegant technique, recently reviewed by Ullrich *et al.*,[17] has been used in a variety of pioneering atomic and molecular physics experiments. Despite the complexity of their spectrometer configuration, the two-dimensional position-sensitive detection system and its timing electronics, is based essentially on a two-field TOF geometry. In order to study photoionization fragmentation processes, Eland[18] and Lavollée[19] have also developed linear two-field TOF systems that similarly map the ion's three momentum components. Moreover, the sophisticated detection system of Lavollée has been used recently to map the momenta of two near-threshold electrons arising from photodouble ionization of helium using the same TOF technique.[20] Other applications of the two-field system in-

[a]Electronic mail: d.p.seccombe@newcastle.ac.uk
[b]Electronic mail: t.j.reddish@ncl.ac.uk

clude the determination of free energies and rate constants associated with the dissociation of molecular ions,[21,22] the detection of large molecular clusters[23] and the imaging of the angular distributions of state-selected photodissociation products.[24,25]

The general mathematical relations pertaining to space focusing that are presented here build upon the previously mentioned pioneering work of Wiley and McLaren[15] using a two-field system which has been more recently extended to second order by Conover *et al.*[23] and Eland.[26] However, a different—although obviously related—set of defining parameters will be adopted, which more readily lend themselves for extension to *m* fields and/or *n*-order space focusing. The merits of introducing the extra complexity will also be discussed. To place things in context, we will briefly review the one- and two-field situations before presenting the general case, which although complicated has a straightforward, solvable form. It is interesting, therefore, to note that Srivastava, Iga, and Rao[27] have ''segmented'' their drift tube into several cylinders held at different potentials, thereby improving the mass and energy resolution. This work puts the multifield aspect of that design on a firmer theoretical basis and provides insight as to what parameters should be optimized in future designs.

II. THEORY

A. Space focusing

A conventional linear time-of-flight mass spectrometer consists of cylindrically symmetric accelerating sections followed by a constant-velocity—or ''drift''—region, as shown in Fig. 1. Acceleration of the ions is caused by uniform electric fields that act along the direction of the symmetry axis. The most basic TOF system utilizes one electric field [Fig. 1(a)], and in this case the ion time of flight (T_1) and its terminal velocity (v_1) are simply given by

$$T_1=\frac{v_1-u_0}{a_1}+\frac{D_2}{v_1}, \tag{1}$$

$$v_1=(u_0^2+2a_1D_1)^{1/2}, \tag{2}$$

where u_0 is the initial on-axis velocity (component) of the ion, a_1 is the acceleration produced by the electric field (E_1) in the source region, D_2 is the length of the field-free region, and D_1 here is the distance the ion travels to the drift region entrance. The acceleration is linearly related to the electric field in the first region, i.e., $a_1=ZeE_1/Mm$ [or $a_i=ZeE_i/Mm$ in the general case (obviously, the general acceleration expression also allows for a simple transformation of the equations for use with electrons/positrons and highly charged ions)], where *m* here is the atomic mass unit and *Z* and *M* are the ionic charge and mass numbers, respectively.

Ions starting from a general position $D_1=\bar{D}_1+z$, where $\bar{D}_1$ is the distance to the center of the source, will have a slightly different time of flight from that corresponding to $\bar{D}_1$. The deviations in the TOF, $\Delta T=T(D_1)-T(\bar{D}_1)$, can be expressed as a Taylor series in the *m*-field case:

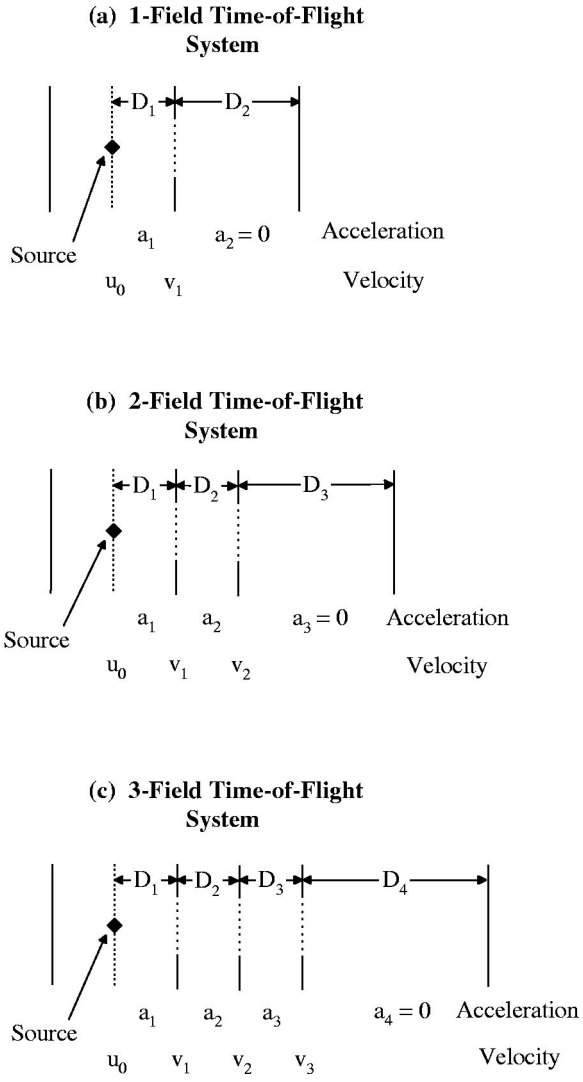

FIG. 1. Schematic diagrams of the one to three electric-field TOF configurations along with the basic definitions of the lengths, velocities, and accelerations used in the mathematical derivations. The source region is indicated and u_0 corresponds to the initial velocity (component) along the TOF axis. The velocities v_i correspond to the axial speed at the end of the *i*th accelerating region. From the trends indicated, it is straightforward to extrapolate our nomenclature to four-, five-, or even *m*-field configurations.

$$\Delta T=\sum_{n=1}^{\infty}\left(\frac{d^nT_m}{dD_1^n}\right)_{\bar{D}_1}\frac{(z)^n}{n!}. \tag{3}$$

In practice, any interaction region will have a finite size, characterized in this work by a half-width *s*, hence space focusing requires mechanical and electric-field arrangements that result in as many of the derivatives as possible in Eq. (3) being set to zero. A ''first-order'' space focus is achieved by setting the first derivative to zero, while a ''second-order'' space focus, for example, is achieved by setting both $(dT/dD_1)_{\bar{D}_1}$ and $(d^2T/dD_1^2)_{\bar{D}_1}$ to zero.

Returning to the one-field TOF design, one can easily show that for $u_0=0$ (the initial condition that is usually assumed in space-focusing design) the $(dT/dD_1)_{\bar{D}_1}=0$ condition results in the constraint: $L_2=D_2/\bar{D}_1=2$. Thus when $u_0=0$ first-order space focusing is simply fixed by the appa-

ratus geometry, independent of the strength of the electric field. However, since $(d^2T/dD_1^2)_{\bar{D}_1}=0$ requires $L_2=2/3$, it is not possible to set simultaneously the first two terms in Eq. (3) to equal zero. Second—and higher—order space-focusing conditions require more acceleration regions in the TOF design.

The commonly used two-field TOF system [Fig. 1(b)] has similar time and terminal velocity equations corresponding to Eqs. (1) and (2):

$$T_2=\frac{v_1-u_0}{a_1}+\frac{v_2-v_1}{a_2}+\frac{D_3}{v_2}, \tag{4}$$

$$v_2=(u_0^2+2a_1D_1+2a_2D_2)^{1/2}, \tag{5}$$

where v_1 is still given by Eq. (2). In evaluating the derivatives, it is more useful to adopt certain dimensionless quantities as these turn out to be the most appropriate parameters in space-focusing design. In the two-field case we make the substitutions: $R_2=E_2/E_1$, $L_2=D_2/D_1$, and $L_3=D_3/D_1$ (generally, $R_i=E_i/E_1$ and $L_i=D_i/D_1$), and show that

$$\frac{v_2^2}{2a_1D_1}=\frac{u_0^2+2a_1D_1+2a_2D_2}{2a_1D_1}$$

$$=\frac{u_0^2}{2a_1D_1}+1+R_2L_2=X+R_2L_2, \tag{6}$$

where $X=1$ when $u_0=0$. Therefore,

$$\left(\frac{v_2}{v_1}\right)^2=\frac{v_2^2}{2a_1D_1}\frac{2a_1D_1}{v_1^2}=\frac{X+R_2L_2}{X}=1+\frac{R_2L_2}{X}=K_2. \tag{7}$$

The physical significance of the dimensionless quantity K_2 is that it is equal to the square of the ratio of the ion's axial momentum after the second field to that at the exit of the first extraction field. More usefully, K_2 (in general, K_m) is employed to minimize the complexity of the subsequent equations. Second-order focusing requires both $(dT/dD_1)_{\bar{D}_1}$ and $(d^2T/dD_1^2)_{\bar{D}_1}$ to be zero, which can be shown to be satisfied by the following two simultaneous equations:

$$2XK_2\left[(K_2)^{0.5}\left(1-\frac{1}{R_2}\right)+\frac{1}{R_2}\right]-L_3=0, \tag{8}$$

$$2XK_2\left[(K_2)^{1.5}\left(1-\frac{1}{R_2}\right)+\frac{1}{R_2}\right]-3L_3=0. \tag{9}$$

It is important to recognize that although there are five experimental variables (E_1,E_2,$\bar{D}_1$,D_2, and D_3) in the two-field case it is the *ratios* of electric-field strengths and the lengths, all with respect to the first acceleration region, that appear in space-focusing conditions (8) and (9). First-order focusing requires only the constraint of Eq. (8); therefore, there exists the freedom to set the values of two parameters (e.g., L_2 and L_3) and the third (R_2) is fixed appropriately. In second-order space focusing, however, only one parameter can independently be assigned a value, since the other two then follow from Eqs. (8) and (9). At the present time, the two-field TOF mass spectrometer is very widely used, and in many cases only first-order space focusing is required. There are enough parameters to satisfy this condition and still have flexibility in operation. Even second-order space focusing is reasonably straightforward to obtain, in principle, although in Sec. III A we will show that in order for the benefits of space focusing to be fully realized, the accuracy of the parameters (i.e., the R_2, L_2, and L_3 ratios) must be better than ~0.1%–1%. If tuning the electric fields can compensate for any errors in these values, then the space-focus condition can be achieved in practice. If, however, there is a dimensional constraint—as in the two-field case tuned for a second-order focus (since L_2 and L_3 are coupled)—the space-focus condition is not straightforward, since it is virtually impossible to construct the apparatus to the required accuracy.

The general experimental need for a more sophisticated TOF design—yet still based on simple uniform electric fields—and the relative simplicity of Eqs. (8) and (9) prompted us to search for the general relations for an *m*-field TOF system with *n*-order space focusing. As before, the TOF equation is simply the sum of the times spent in each region, which can be generalized to the *m*-field case to be

$$T_m=\frac{v_1-u_0}{a_1}+\sum_{i=2}^{m}\frac{v_i-v_{i-1}}{a_i}+\frac{D_{m+1}}{v_m}. \tag{10}$$

Similarly, the velocity after traversing the mth field is given by

$$v_m=\left(u_0^2+\sum_{i=1}^{m}2a_iD_i\right)^{1/2}, \tag{11}$$

or, more usefully,

$$\left(\frac{v_m}{v_1}\right)^2=1+\sum_{i=2}^{m}\frac{R_iL_i}{X}=K_m, \tag{12}$$

where, as in Eq. (7),

$$X=1+\frac{u_0^2}{2a_1D_1}=1+\frac{Mmu_0^2}{2D_1ZeE_1}=1+\frac{U_0}{D_1E_1}. \tag{13}$$

Equation (13) reveals a particularly important property of the general space-focusing condition, namely, that it is dependent on the ion's ''axial'' velocity (i.e., due to the velocity component along the TOF axis). For the purpose of the present discussion, the $X=1$ condition is imposed. Hence, although the space-focus conditions do not depend explicitly on the magnitudes of E_1 and $\bar{D}_1$, their values will affect the legitimacy of this approximation. In particular, E_1 and $\bar{D}_1$ must be set to ensure $u_0^2/2a_1\bar{D}_1$is close to zero, which suggests that space focusing will work best for low-energy ions [i.e., $U_0(eV)\ll\bar{D}_1E_1$].

In an *m*-field system ($m>2$), there exists a general set of *n* simultaneous equations that need to be solved for the *n*th-order focusing condition, i.e., $\{(d^jT/dD_1^j)_{\bar{D}_1}=0\}_{j=1\rightarrow n}$. The set, expressed in terms of the parameters of the TOF system, can be simplified to

$$\left\{2XK_m\left[\frac{1}{R_m}+K_m^{j-1/2}\left(1-\frac{1}{R_2}\right)+\sum_{i=2}^{m-1}\left(\frac{K_m}{K_i}\right)^{j-1/2}\times\left(\frac{1}{R_i}-\frac{1}{R_{i+1}}\right)\right]-(2j-1)L_{m+1}=0\right\}_{j=1\to n}. \tag{14}$$

This set depends on R_k, L_k ($k=2$ to m in steps of 1) and L_{m+1}; the total number of these variables is then equal to $(2m-1)$. Since the number of equations in the set that can be satisfied simultaneously is equal to the number of parameters, the highest order of the space-focus condition ($n_{\max}$) that can be achieved is given by $n_{\max}=2m-1$. It should be noted, however, that for all cases with $m>1$, the maximum order of space focus can only be achieved by setting L_{m+1} to zero. For example, in the previously discussed two-field case, third-order focusing should be technically possible. However, the third-order solution occurs when either $L_3=0$, $L_2=-1$, $R_2=1$ or $L_3=0$, $L_2=1$, $R_2=-1$; the first is unphysical and the second results in a terminal velocity of zero for ions starting at $\bar{D}_1$, and ions from $D_1<\bar{D}_1$ never reach the detector. Thus, for $m>1$ only a space-focus order as high as $2m-2$ is potentially useful in practice. Even so, the technical difficulties in achieving that highest $(2m-2)$th order condition are severe, as we indicated earlier in the two-field case. Consequently, since $m-1$ is the number of adjustable electric-field ratios, space focusing would be more reliably achieved in a design if one considered $m-1$ to be the highest practicable order.

In the case of a three-field system [see Fig. 1(c)], the parameters are R_2, R_3, L_2, L_3, and L_4 and the set of equations derived from Eq. (14) for $j=1-4$ are, respectively,

$$2XK_3\left[(K_3)^{0.5}\left(1-\frac{1}{R_2}\right)+\left(\frac{K_3}{K_2}\right)^{0.5}\left(\frac{1}{R_2}-\frac{1}{R_3}\right)+\frac{1}{R_3}\right]-L_4=0, \tag{15}$$

$$2XK_3\left[(K_3)^{1.5}\left(1-\frac{1}{R_2}\right)+\left(\frac{K_3}{K_2}\right)^{1.5}\left(\frac{1}{R_2}-\frac{1}{R_3}\right)+\frac{1}{R_3}\right]-3L_4=0, \tag{16}$$

$$2XK_3\left[(K_3)^{2.5}\left(1-\frac{1}{R_2}\right)+\left(\frac{K_3}{K_2}\right)^{2.5}\left(\frac{1}{R_2}-\frac{1}{R_3}\right)+\frac{1}{R_3}\right]-5L_4=0, \tag{17}$$

$$2XK_3\left[(K_3)^{3.5}\left(1-\frac{1}{R_2}\right)+\left(\frac{K_3}{K_2}\right)^{3.5}\left(\frac{1}{R_2}-\frac{1}{R_3}\right)+\frac{1}{R_3}\right]-7L_4=0. \tag{18}$$

First-order space focusing is achieved by finding a set of parameters which satisfies Eq. (15), for second-order, Eqs. (15) and (16); for third-order, Eqs. (15)–(17); and for fourth-order, Eqs. (15)–(18). Those equations can be solved numerically for the sets of parameters using standard mathematical software, such as MATHCAD or MATHEMATICA. However, in optimizing the design there are other considerations which may have an effect on which set of solutions are adopted. The space and velocity contributions to the mass resolution are two such criteria, and it is to them that we now turn.

B. Mass resolution

The mass resolution of a TOF mass spectrometer is simply related to its capability to separate adjacent mass numbers. This in turn depends on (a) the size of the interaction region and the space-focusing order and (b) the axial velocity distribution of the ions. Combining the two effects is extremely complicated (see Refs. 28 and 29), but following Wiley and McLaren,[15] we will treat the effects independently and then compare their contributions to the overall resolution.

The ion time of flight given in Eq. (10) is directly proportional to $\sqrt{M}$ when $u_0=0$, a relation that is valid regardless of the number of electric-field regions in the design. Thus, the time separation for adjacent masses ($\Delta M=1$) is given by

$$T_{M+1}-T_M=T_M\left[\left(\frac{M+1}{M}\right)^{1/2}-1\right]=T_M\left[\left(1+\frac{1}{M}\right)^{1/2}-1\right]\approx\frac{T_M}{2M}. \tag{19}$$

A measure of the space resolution M_s is the maximum value of the mass number M, for which

$$\Delta T_s\leqslant(T_{M+1}-T_M)=\frac{T_M}{2M}, \tag{20}$$

where ΔT_s corresponds to the difference between opposite extremes of the ion TOF peak. This can be obtained using Eq. (3) for a specific space-focused TOF design and interaction region size. In order to evaluate that expression, one needs the general form of the jth derivative, which is related to Eq. (14) and is given explicitly by

$$\frac{d^jT}{dD_1^j}=\left[\frac{a_1^jD_1(-1)^{j+1}}{v_m^{2j+1}}\right]\left\{2XK_m\left[\frac{1}{R_m}+K_m^{j-1/2}\left(1-\frac{1}{R_2}\right)+\sum_{i=2}^{m-1}\left(\frac{K_m}{K_i}\right)^{j-1/2}\left(\frac{1}{R_i}-\frac{1}{R_{i+1}}\right)\right]-(2j-1)L_{m+1}\right\}. \tag{21}$$

The first term of Eq. (21) is only zero in unphysical situations, (i.e., if any of the following are true: $a_1=0$, $D_1=0$, $v_m=\infty$) and was, therefore, excluded from Eq. (14). Some caution should be applied when using Eq. (21) in Eq. (3), since the applicable range of length deviation z from $\bar{D}_1$ is small and depends on the order of space focusing employed. For a given design, it is more reliable to evaluate ΔT_s directly by determining T using Eq. (10) across the interaction region. More significantly, the TOF deviations ΔT, as a function of $D_1=\bar{D}_1-z\to\bar{D}_1+z$, have a shape that depends on the *order* of space focusing, regardless of the number of electric fields used. In general, the odd-numbered orders display a nearly symmetric profile, whereas the even orders have an antisymmetric shape with a point of inflection at $\bar{D}_1$

(this is later illustrated in Fig. 6). This means the overall time spread across the interaction region is $\sim 2\Delta T(\overline{D_1}+s)$ for even orders, but is only $\sim \Delta T(\overline{D_1}+s)$ for odd-order focusing. Consequently, while in general one can achieve about an order of magnitude reduction in the time spread by going to the next-higher-order space focusing, a greater improvement will arise when going from an even- to an odd-order condition, rather than vice versa. This will be demonstrated quantitatively in Sec. III C.

As mentioned earlier, the axial velocity distribution of the ions will contribute significantly to the overall TOF resolution since T depends on u_0 [see Eq. (10)]. Initial nonaxial velocities, however, make no contribution to T and, hence, do not affect the resolution. To investigate the effect of the initial velocity, it is convenient to consider two ions of the same mass formed at the same position D_1 with equal but opposite initial velocities. The ion that moves away from the detection system is decelerated until it stops, due to E_1, and then is accelerated back towards the detector. When it returns to D_1 it will have attained the same initial velocity as the other ion, and so the TOF from that point onwards will be the same. Thus, the time spread is due to the ''turn around'' time of the ion. By substituting $u_0=+u,-u$ into Eq. (10), one can easily show that the turn around time ΔT_{u_0} is

$$\Delta T_{u_0}=\frac{2|u_0|}{a_1}=\frac{2|u_0|mM}{ZeE_1}, \tag{22}$$

which is independent of the initial position, D_1. The mass resolution from this effect can be treated in an analogous way to the space-focusing contribution using Eq. (20), i.e.,

$$M_{u_0}\approx T/2\Delta T_{u_0}, \tag{23}$$

where T is evaluated using Eq. (10) with $u_0=0$. Substituting the dimensionless parameters we introduced for the space-focusing analysis into Eq. (23) results in

$$M_{u_0}=\frac{1}{4}\left\{\left(\frac{X}{X-1}\right)^{0.5}\left[\left(1-\frac{1}{R_2}\right)+\frac{K_2^{0.5}}{R_2}+\frac{L_3}{2XK_2^{0.5}}\right]\right\}, \tag{24}$$

for the two-field case. In the general m-field case ($m>2$), M_{u_0} can be shown to be given by the following analytical form:

$$M_{u_0}=\frac{1}{4}\left\{\left(\frac{X}{X-1}\right)^{0.5}\left[\left(1-\frac{1}{R_2}\right)+\sum_{i=2}^{m-1}K_i^{0.5}\left(\frac{1}{R_i}-\frac{1}{R_{i+1}}\right)+\frac{K_m^{0.5}}{R_m}+\frac{L_{m+1}}{2XK_m^{0.5}}\right]\right\}. \tag{25}$$

This expression provides useful insight into how the experimental parameters affect the value of M_{u_0}. Although M_{u_0} is dependent on all the experimental variables u_0, D_i, R_i, it can be shown that the L_{m+1} term, pertaining to the length of the field-free section, is by far the most significant. The overall expression, however, is dominated by the $\sqrt{X/(X-1)}$ factor, since as $u_0\rightarrow 0$, $X\rightarrow 1$, and so, $M_{u_0}\rightarrow\infty$; this is expected from first principles and is evident in Eqs. (22) and (23). Thus, minimizing the axial velocity distribution is *crucial* for obtaining a high mass resolution. This can be reduced very effectively by, for example, the use of supersonic expansions for the gas source and configuring the TOF axis to be orthogonal to the molecular-beam direction. In circumstances where the parent ion dissociates, however, the velocity distribution of the fragment ions may necessarily be large, and so provide a fundamental limit on the mass resolution. Once $|u_0|$ has been minimized by appropriate experimental methods, its remaining effect on the mass resolution is further countered by increasing the acceleration (a_1)—and the distance traveled ($\overline{D_1}$)—in the first region [see Eq. (13)]. The choice of the electric-field strength (E_1) is, therefore, important, which obviously affects the magnitudes of the other fields (via R_i) and the corresponding power supply arrangements. So, ultimately, there is an upper limit on the mass number that can be used in practice.

Having reached that limit, the onus is then put back onto optimizing the space focusing and ensuring that the resolutions M_s and M_{u_0} are comparable. It is worth emphasizing that the M_{u_0} value from Eq. (25) is independent of space focusing. To relate the TOF design parameters to both M_s and M_{u_0} requires the set of conditions (14) be solved for $X\neq 0$, but with X being as close to unity as possible. Notice, though, that in Eq. (25), the central summation term, which obviously disappears in the two-field case (24), depends on the *combination* of the electric-field ratios. Thus, the choice of R_i and D_i values used also affects the resolution to some extent. Therefore, in order to uncouple more parameters for a given space-focusing order, and so have flexibility in their choice, an increase in the number of electric fields is generally required.

III. CALCULATION

A. Two-field system

To demonstrate the advantages of using three and four fields, we must first consider the limitations of the conventional two-field linear TOF mass spectrometer [Fig. 1(b)]. To recapitulate, the space-focus-defining variables for this case are R_2, L_2, and L_3. In Sec. II A, we concluded that the highest order one could consider useful in principle is $2m-2$, where m is the number of fields. In the two-field system, therefore, second order is the highest that should be achievable and this can be done by finding a set of values for R_2, L_2, and L_3 that satisfies Eqs. (8) and (9). This was done numerically using MATHCAD 2000™. These solutions are depicted graphically in Fig. 2, where the coupling of any two of the three variables, which should inevitably arise from the satisfaction of the two simultaneous equations, is clearly demonstrated. Since two of the three variables are constrained, and there is only one electric-field ratio (R_2), a dimensional constraint (L_2 depends on L_3) is inevitably associated with a two-field system tuned to second order. In a practical design, thin metal meshes are often used to create the uniform electric fields. These, in turn, produce small perturbations in the field close to the mesh surfaces. Even if meshes are not used, the uniformity of the field across the

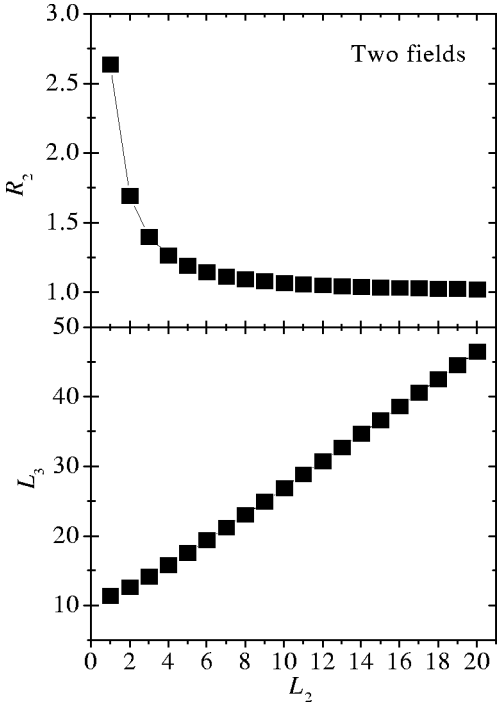

FIG. 2. Second-order space focusing solutions for the dimensionless quantities R_2 and L_3, as a function of L_2, in a two-field system. This demonstrates that it is impossible to choose L_2 and L_3 independently.

active area of the TOF system is unlikely to be within the required accuracy given below. Clearly, the highest possible accuracy associated with the mechanical lengths depends on the overall scale of the design. Having said this, the dimensions of the system cannot usually be controlled to an accuracy of better than ~0.1%–1%. It is, therefore, imperative that we test the sensitivity of the second-order space-focus condition to small variations in either L_2 or L_3. This was done using a trial two-field TOF system (a) configured to second-order focus using the design parameters listed in Table I. The time of flights for ions starting different positions within the interaction region were calculated. The difference between these time of flights and that for an ion originating from the center of the interaction region ($D_1 = \overline{D_1}$) is plotted in Fig. 3 as a function of starting position (D_1). The distance D_2 was then increased by 0.01%, 0.1%, and 1% [TOF systems (b), (c), and (d), respectively, in Table

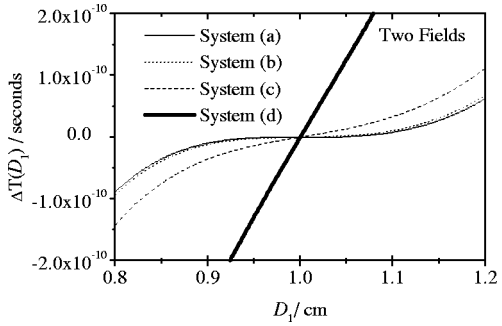

FIG. 3. TOF-variation functions for the two-field systems (a)–(d), whose parameters are given in Table I (see the text for discussion).

I], and the resulting TOF-variation functions are also shown in Fig. 3. Since second-order space focusing results in a point of inflexion at the center of the interaction region (see Fig. 3), the space-focus width ΔT_s can be calculated from $\Delta T_s = T(\overline{D_1}+s) - T(\overline{D_1}-s)$. The mass resolution M_s, which then follows from $T(\overline{D_1})/2\Delta T_s$ [see Eq. (20)], has also been determined for all the systems (see Table I) with interaction region sizes of $s = \pm 1$ and ± 2 mm. The M_s trends as D_2 is perturbed progressively can be compared to the corresponding value obtained when using a first-order design of similar dimensions [system (e) in Table I]. It is clear that if there is only a 1% error in L_2, the mass resolution is reduced by about an order of magnitude and the benefit of second-order space focusing is lost. Since L_2 is coupled to L_3, any errors in L_2 cannot be corrected by solely changing R_2, thus the reduction in M_s cannot be recovered completely. This is a serious practical drawback in the design.

B. Three fields

Therefore, the question arises whether second order can be obtained more easily and reliably in the three-field situation. Here, the space-focus-defining variables are R_2, R_3, L_2, L_3, and L_4. In order to find a set of values for these parameters which satisfy the second-order space-focusing condition, Eqs. (15) and (16) need to be solved numerically. Some of the solutions are presented graphically in Fig. 4, where it is clear that there is no constraint on the mechanical dimensions (L_i). Second-order space focusing fixes two of

TABLE I. Comparison of the mass resolutions (M_s) for a representative two-field TOF system, based on ions initially at rest. Systems (a)–(d) are configured for second-order space focusing, as discussed in the text, but with a systematic error being increasingly introduced to the D_2 value. A first-order space focused two-field system (e) with the same $\overline{D_1}$ and D_3 values is also shown for comparison.

	Two-field TOF systems				
	(a)	(b)	(c)	(d)	(e)
E_1/V cm^{-1}	100	100	100	100	100
E_2/V cm^{-1}	132.14	132.14	132.14	132.14	329.39
$\overline{D_1}$/cm	1	1	1	1	1
D_2/cm	3.4992	3.4992 ×1.0001	3.4992 ×1.001	3.4992 ×1.01	1
D_3/cm	15	15	15	15	15
M_s ($s=\pm 1$ mm)	1.3×10^5	1.0×10^5	3.4×10^4	4.5×10^3	1.2×10^4
M_s ($s=\pm 2$ mm)	1.5×10^4	1.4×10^4	9.3×10^3	2.0×10^3	2.5×10^3

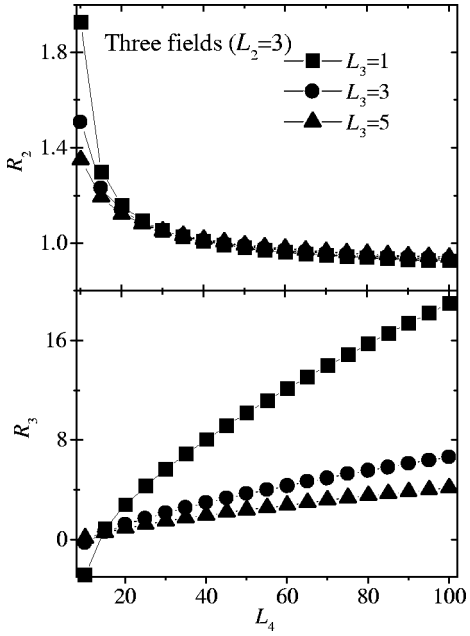

FIG. 4. Some solutions for R_2 and R_3 as a function of L_4 (for selected values of L_3) in a three-field system with second-order space focusing. In all cases $L_2=3$. The freedom to choose L_2, L_3, and L_4 demonstrates the absence of any dimensional constraint.

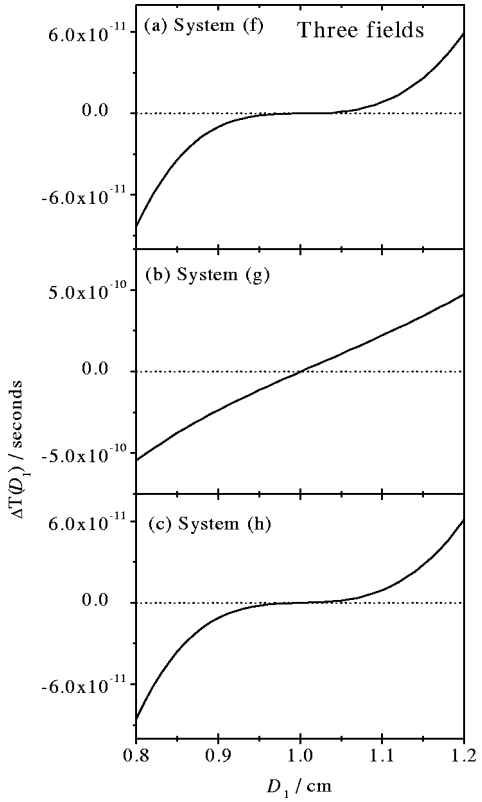

FIG. 5. TOF-variation functions for the three-field systems (f)–(h), whose parameters are given in Table II. The departure from second-order space focusing in system (g) is restored by simply changing the electric fields in system (h), as discussed in the text.

the variables, exactly like the two-field scenario, but here there are *two* electric-field ratios while there exists only one in the two-field TOF design. Hence, the two constrained variables can *both* be electric-field ratios, leaving the mechanical dimensions free. The ''freeing up'' of the length ratios has far-reaching implications for the practical implementation of a space-focus design. To demonstrate this, we consider a three-field TOF system (f), with the parameters listed in Table II and with very similar dimensions to (a), configured to second-order space focus. If D_2 is subjected to a 1% increase [system (g) in Table II], M_s ($s=\pm 2$ mm) falls from 1.7×10^4 to 2.4×10^3, a similar effect to that observed in going from systems (a) to (d) ($1.5\times10^4\rightarrow2.0\times10^3$). In the three-field case, however, since there are no dimensional constraints, the second-order space-focus condition can be regained by simply adjusting E_2 and E_3 to compensate for the increase in D_2. By changing E_2 and E_3 to 127.66 and 45.88 V cm^{-1}, respectively [system (h) in Table II], M_s increases from 2.4×10^3 to 1.7×10^4, and the second-order space-focus condition is regained. The TOF-variation functions for these three cases are shown in Fig. 5. In this example, the error in D_2 was known, so one could recalculate the new values of E_2 and E_3. In a practical situation, one would not know where the error lay, hence, the fields would have to be tuned to optimize the TOF peak full width at half maximum. This operational flexibility is a distinct advantage in using a three-field TOF system for second-order space focusing.

TABLE II. Comparison of the mass resolutions (M_s) for a representative three-field TOF system configured for second-order space focusing and based on ions initially at rest. The small systematic error introduced to the D_2 value in (g) degrades significantly the mass resolution, which is restored in (h) by simply altering the electric fields, as discussed in the text.

	Three-field TOF systems		
	(f)	(g)	(h)
E_1/V cm^{-1}	100	100	100
E_2/V cm^{-1}	127.80	127.80	127.66
E_3/V cm^{-1}	48.77	48.77	45.88
D_1/cm	1	1	1
D_2/cm	3.5	3.5×1.01	3.5×1.01
D_3/cm	1	1	1
D_4/cm	15	15	15
M_s ($s=\pm1$ mm)	1.4×10^5	5.3×10^3	1.4×10^5
M_s ($s=\pm2$ mm)	1.7×10^4	2.4×10^3	1.7×10^4

We now ask whether higher orders can be obtained in the three-field case. In principle, space focusing up to the fourth order should be achievable. The familiar problem, however, of constrained dimensions arises for third- and fourth-order space focusing, since there exist only two electric-field ratios. Hence, we believe that it is not realistic to expect to obtain these higher-order space-focusing conditions using a three-field TOF system and it is simpler to employ more fields to achieve the same aim. The conclusions drawn for the two- and three-field systems are in line with the assertion in Sec. II A that $m-1$ is the highest practicable order that one should consider.

C. Four fields

In the previous section, we concluded that if third-order space focusing is required, a four-field device would be easier to configure than a three-field device. We will now

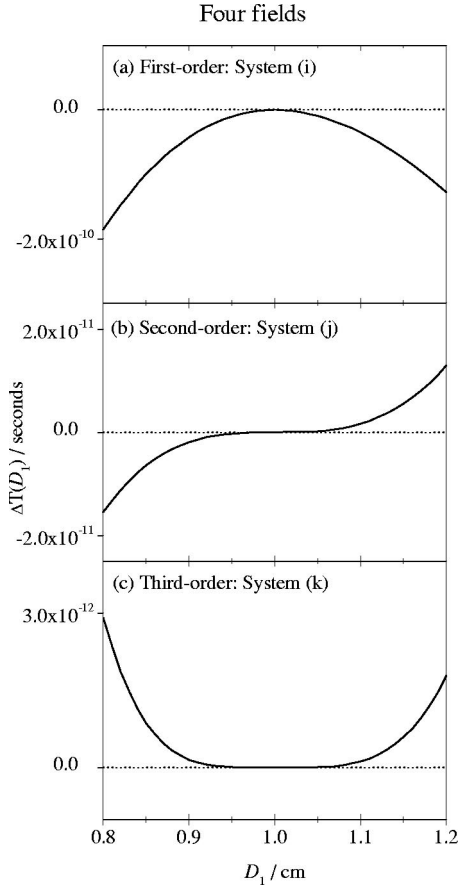

FIG. 6. TOF-variation functions for four-field TOF systems configured to (a) first-order, (b) second-order, and (c) third-order space focusing, corresponding to systems (i)–(k) in Table III. Note the change in the *y*-axis scales and the symmetry of the profiles with order.

investigate the benefits of third-order space focusing in terms of the overall mass resolution by comparing the TOF systems (i)–(k) tuned, respectively, to first-, second-, and third-order space focusing, see Fig. 6. The dimensions of the three four-field systems are identical and the values of the space-focus-defining parameters are listed in Table III. Unfortunately, the mass resolutions calculated for these four-field systems cannot be compared directly with those of the two- and three-field systems listed in Tables I and II. This is because third-order solutions in the four-field geometry require L_5 to be at least ~30. Nevertheless, the effect of the transitions from first to second to third-order space focusing, within the four-field regime, can still be demonstrated. Using the larger of the two interaction regions ($s=\pm 2$ mm), the values for M_s associated with systems (i)–(k) are 1.8×10^4, 1.2×10^5, and 1.1×10^6. As expected, M_s increases with each order of space focus by approximately an order of magnitude.

In designing a TOF mass spectrometer, one should also consider the effect that the initial axial velocity distribution has on the overall mass resolution. There is clearly no point tuning a spectrometer to a higher order of space focus if M_s is already more than an order of magnitude higher than M_{u_0}. In this case, efforts should be made to minimize the effects of the velocity distribution if possible. Values for M_{u_0} associated with systems (i)–(k) are also listed in Table III. The

TABLE III. Comparison of the mass resolutions due to space focusing (M_s) and the axial velocity distribution, M_{u_0} for a representative four-field TOF system. Systems (i)–(k) all have the same dimensions and are configured for first-, second-, and third-order space focusing, respectively.

	Four-field TOF systems		
	(i)	(j)	(k)
E_1/V cm^{-1}	100	100	100
E_2/V cm^{-1}	100	100	90.66
E_3/V cm^{-1}	200	134.61	217.98
E_4/V cm^{-1}	127.24	191.28	122.04
D_1/cm	1	1	1
D_2/cm	1	1	1
D_3/cm	2	2	2
D_4/cm	3	3	3
D_5/cm	30	30	30
M_s ($s=\pm1$ mm)	7.8×10^4	9.2×10^5	2.1×10^7
M_s ($s=\pm2$ mm)	1.8×10^4	1.2×10^5	1.1×10^6
M_{u_0} (2.6×10^{-2} eV)	1.2×10^2	1.1×10^2	1.1×10^2
M_{u_0} (8.6×10^{-8} eV)	2.2×10^3	1.9×10^3	1.9×10^3
M_{u_0} (8.6×10^{-11} eV)	6.8×10^4	6.1×10^4	6.1×10^4
M_{u_0} (8.6×10^{-13} eV)	2.2×10^6	1.9×10^6	1.9×10^6

energies considered are 2.6×10^{-2}, 8.6×10^{-5}, 8.6×10^{-8}, and 8.6×10^{-11} eV, corresponding to temperatures of 300, 1, 1×10^{-3}, and 1×10^{-6} K, respectively. It is clear from Table III that if the interaction region is considered to have dimensions $s=\pm2$ mm, no significant improvement in the overall mass resolution will be realized in going from first to second orders at room temperature (300 K) for a TOF apparatus of this overall length. At 1 K, a transverse temperature now routinely achieved in molecular beams, there is a good case for configuring the system to second order since in system (i) M_{u_0} is only ~8 times lower than M_s. However, as we have already said, combining the two effects together to yield the overall resolution is rather an involved task and has not been attempted in this study. At 1 mK and below, third-order space focusing should be employed.

IV. DISCUSSION

Using the ideas arising from this study, the following conclusions can now be drawn regarding the design of linear TOF mass spectrometers.

(1) The space-focus contribution to the overall mass resolution should be approximately an order of magnitude lower than that arising from the initial on-axis velocity distribution. If it has a greater contribution than this, then a significant improvement to the mass resolution will occur if the system is tuned to a higher order of space focus.

(2) The technology associated with the ionization of cold gas targets is now advanced enough that second-order space focusing is essential. At some point in the future, third-order focusing may well be beneficial.

(3) The number of fields employed in the TOF system should ideally not be lower than $n+1$, where n is the order of space focus required. Thus, second-order space focusing requires three fields; third order needs four fields.

(4) While the space focus condition itself does not depend on the absolute values of E_1 and $\overline{D_1}$ when $X=1$, this approximation relies on the energies of the ions being much

smaller than the $\overline{D}_1 E_1$ product. Hence, the extraction field (E_1) should be as high as practically possible. This, in turn, affects the values of the other fields and obviously shortens the overall ion time of flight. Consequently, this places more stringent demands on the timing resolution, dynamic range, and dead time of the electronics. Increasing E_1 also results in higher collection efficiency and a lower velocity contribution to the mass resolution.

It is debatable whether the practical implementation of all the ideas in this article will result in a significant improvement in the TOF mass resolution at the present time. This largely depends on the specific application and the overall length of the TOF system employed. Nevertheless, the realization of *second-order* space focusing is certainly important, which up until now has generally been attempted using two fields. In this study, we have demonstrated that this order of space focusing can most easily and reliably be achieved if three or more fields are used. Laser-cooling methods may further benefit from the use of third-order space focusing using four electric fields. In conclusion, we anticipate that the relations derived here will significantly influence the design of future linear TOF mass spectrometers.

ACKNOWLEDGMENTS

One of the authors (D.P.S.) gratefully acknowledges EPSRC for his PDRA position. The authors also thank Tom Field and Barry Fisher for their critical reading of the manuscript and Stephen Collins for his assistance with some of the calculations.

[1] J. M. B. Bakker, Int. J. Mass Spectrom. Ion Phys. **6**, 291 (1971).
[2] W. P. Poschenrieder, Int. J. Mass Spectrom. Ion Phys. **6**, 413 (1971).
[3] W. P. Poschenrieder, Int. J. Mass Spectrom. Ion Phys. **9**, 357 (1972).
[4] B. A. Mamyrim, V. I. Karataev, D. V. Shmikk, and V. A. Zagulin, Sov. Phys. JETP **37**, 45 (1973).
[5] T. Bergmann, T. P. Martin, and H. Schaber, Rev. Sci. Instrum. **61**, 2592 (1990).
[6] W. S. Crane and A. P. Mills, Rev. Sci. Instrum. **56**, 1723 (1985).
[7] L. D. Hulett, Jr., D. L. Donohue, and T. A. Lewis, Rev. Sci. Instrum. **62**, 2131 (1991).
[8] N. L. Marable and G. Sanzone, Int. J. Mass Spectrom. Ion Phys. **13**, 185 (1974).
[9] J. A. Browder, R. L. Miller, W. A. Thomas, and G. Sanzone, Int. J. Mass Spectrom. Ion Phys. **37**, 99 (1981).
[10] D. J. Trevor, L. D. Van Woerkom, and R. R. Freeman, Rev. Sci. Instrum. **60**, 1051 (1989).
[11] D. Price and G. J. Milnes, Int. J. Mass Spectrom. Ion Processes **99**, 1 (1990).
[12] J. Kissell, Adv. Mass Spectrom. **10**, 175 (1986).
[13] K. B. Davis, M. O. Mewes, M. R. Andrews, N. J. van Druten, D. S. Durfee, D. M. Kurn, and W. Ketterle, Phys. Rev. Lett. **75**, 3969 (1995).
[14] J. N. Ullom, M. Frank, J. M. Horn, S. E. Labov, K. Langray, and W. H. Benner, Nucl. Instrum. Methods Phys. Res. A **444**, 385 (2000).
[15] W. C. Wiley and I. H. McLaren, Rev. Sci. Instrum. **76**, 1150 (1955).
[16] R. Moshammer, M. Unverzagt, W. Schmitt, J. Ullrich, and H. Schmidt-Böcking, Nucl. Instrum. Methods Phys. Res. B **108**, 425 (1996).
[17] J. Ullrich, R. Moshammer, R. Dorner, O. Jagutzki, V. Mergel, H. Schmidt-Böcking, and L. Speilberger, J. Phys. B **30**, 2917 (1997).
[18] J. H. D. Eland, Meas. Sci. Technol. **5**, 1501 (1994).
[19] M. Lavollée, Rev. Sci. Instrum. **70**, 2968 (1999).
[20] A. Huetz and J. Mazeau, Phys. Rev. Lett. **85**, 530 (2000).
[21] T. Baer, Annu. Rev. Phys. Chem. **40**, 637 (1989).
[22] P. B. Armentrout and T. Baer, J. Phys. Chem. **100**, 12866 (1996).
[23] C. W. S. Conover, Y. J. Twu, Y. A. Yang, and L. A. Bloomfield, Rev. Sci. Instrum. **60**, 1069 (1989).
[24] D. W. Chandler and P. L. Houston, J. Chem. Phys. **87**, 1445 (1987).
[25] T. Kinugawa and T. Arikawa, Rev. Sci. Instrum. **63**, 3599 (1992).
[26] J. H. D. Eland, Meas. Sci. Technol. **4**, 1522 (1993).
[27] S. K. Srivastava, I. Iga, and M. V. V. S. Rao, Meas. Sci. Technol. **6**, 1379 (1995).
[28] J. L. Franklin, P. M. Hierl, and D. A. Whan, J. Chem. Phys. **47**, 3148 (1967).
[29] R. B. Opsal, K. G. Owens, and J. P. Reilly, Anal. Chem. **57**, 1884 (1985).